Analyst

Cite this: *Analyst*, 2011, **136**, 77

www.rsc.org/analyst

**PAPER**

# A low-cost, simple, and rapid fabrication method for paper-based microfluidics using wax screen-printing†

**Wijitar Dungchai,[a] Orawon Chailapakul*[ab] and Charles S. Henry*[c]**

***Received 16th June 2010, Accepted 7th August 2010***
**DOI: 10.1039/c0an00406e**



Wax screen-printing as a low-cost, simple, and rapid method for fabricating paper-based microfluidic devices (μPADs) is reported here. Solid wax was rubbed through a screen onto paper filters. The printed wax was then melted into the paper to form hydrophobic barriers using only a hot plate. We first studied the relationship between the width of a hydrophobic barrier and the width of the original design line. We also optimized the heating temperature and time and determined the resolution of structures fabricated using this technique. The minimum width of hydrophilic channel and hydrophobic barrier is 650 and 1300 μm, respectively. Next, our fabrication method was compared to a photolithographic method using the reaction between bicinchoninic acid (BCA) and $Cu^{1+}$ to demonstrate differences in background reactivity. Photolithographically defined channels exhibited a high background while wax printed channels showed a very low background. Finally, the utility of wax screen-printing was demonstrated for the simultaneous determination of glucose and total iron in control human serum samples using an electrochemical method with glucose oxidase and a colorimetric method with 1,10-phenanthroline. This study demonstrates that wax screen-printing is an easy-to-use and inexpensive alternative fabrication method for μPAD, which will be especially useful in developing countries.

## Introduction

μPADs were recently introduced as alternative devices for point-of-care testing because they have attractive features including low cost, ease of use, low consumption of reagent and sample, portability, and disposability.[1] Several fabrication methods for μPADs have been reported including photolithography,[2–8] polydimethylsiloxane (PDMS) plotting,[9] inkjet etching,[10] plasma etching,[11] cutting,[12] and wax printing.[13] Each fabrication method has its own advantages and limitations. The first reported method was based on photolithography and provided high resolution between hydrophilic and hydrophobic areas (~200 μm of minimal barrier line width).[4] However, this method requires organic solvents, expensive photoresists, and photolithography equipment. An oxygen plasma treatment is also required to create hydrophilic areas. The PDMS plotting method does not need organic solvent and expensive photoresists and also overcomes the problem of physical inflexibility of devices made using photolithography. Unfortunately, this method requires a customized plotter.[9] The inkjet etching method allowed for the simultaneous creation of patterned substrates and the dispensing of chemical reagents. However, this method requires a customized and potentially expensive inkjet printer.[10] Most recently, a wax printing method utilizing a commercially available wax printer was reported for the production of μPADs.[13] Although wax printing has a lower resolution than photolithography (~850 μm of minimal barrier line width), the hydrophilic areas are never exposed to photoresists or other polymers; hence, wax printing methods do not require external processing steps to create the hydrophilic areas. This method does, however, require an expensive wax printer and the accompanying consumables.

One common limitation of the aforementioned fabrication methods is the need for tools that are rare in laboratories of developing countries such as spin coaters, plasma oxidizers, and wax printers.[1] Moreover, trained personnel are required to use and maintain these tools. The aim of this study was to develop low-cost, simple, and rapid fabrication methods requiring minimal external instrumentation for implementation in developing countries. Our proposed fabrication method consists of two simple steps: (1) printing patterns of solid wax on the surface of paper using a simple screen-printing method and common household supplies, and (2) melting the wax into paper to form complete hydrophobic barriers using a hot plate. The overall approach is shown schematically in Fig. 1. Screen printing is

[a]*Electrochemical Research Group, Department of Chemistry, Faculty of Science, Chulalongkorn University, Patumwan, Bangkok, 10330, Thailand*
[b]*National Center of Excellence for Petroleum, Petrochemicals, and Advanced Materials, Chulalongkorn University, Patumwan, Bangkok, 10330, Thailand*
[c]*Department of Chemistry, Colorado State University, Fort Collins, CO, 80523-1872, USA. E-mail: chuck.henry@colostate.edu; Fax: +1-970-491-1801; Tel: +1-970-491-2852*

† Electronic supplementary information (ESI) available: Additional details on the fabrication methods and results. See DOI: 10.1039/c0an00406e

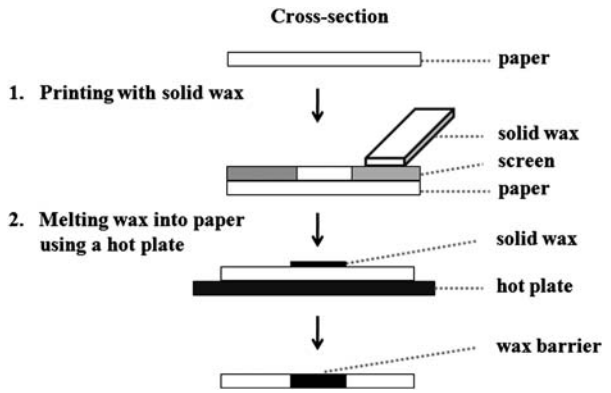


**Fig. 1** Schematic diagram of the fabrication step for wax screen-printing method.

a well-known, inexpensive method for printing images on clothing and other everyday materials as well as creating electrodes.[14–16] Printing screens are cheap (~$5 US or 200 Thai Baht per 100 $cm^2$) and widely available around the world. In addition, wax is inexpensive, can be purchased anywhere in the world, and is environmentally friendly. Finally, the wax screen-printing method is accomplished without the use of a clean room, UV lamp, organic solvents, or sophisticated instrumentation. Another advantage of our method over previous methods is that it requires only a hot plate (or similar heated surface) making it ideal for fabrication of μPADs in developing countries. We first studied the spreading of wax in paper and determined the minimum dimensions achievable for the width of hydrophobic barriers and hydrophilic channels. Next, we studied the background reactivity of wax *versus* photolithography methods, and demonstrated a clear reduction in background signal when using the wax printing method. Finally, applications of colorimetric and electrochemical detection on patterned paper using the wax screen-printing method are presented.

## Experimental

### Materials and equipment

D-(+)-Glucose (99.5%) and glucose oxidase (from *Aspergillus niger*, 215 U $mg^{-1}$) were purchased from Sigma-Aldrich (St Louis, MO). Ascorbic acid (AR grade) was obtained from Mallinckrodt Baker Inc. (Paris, KY). 1,10-Phenanthroline monohydrate (ACS grade) was purchased from Acros organics (Morris Plains, NJ). Potassium phosphate (ACS grade), iron chloride hexahydrate ($FeCl_3 \cdot 6H_2O$, ACS grade), and calcium nitrate (ACS grade) were obtained from Fisher Scientific (Pittsburgh, PA). The bicinchoninic acid (BCA) assay kit was purchased from Pierce (Rockford, IL). Solid wax was obtained from a local candle making supply shop. Whatman #1 filter paper was purchased from Cole-Parmer (Vernon Hills, IL). Carbon ink mediated with Prussian blue (C2070424D2) was purchased from Gwent group (Torfaen, UK). Silver chloride ink (Electrodag 7019) was obtained from Acheson Colloids Company (Port Huron, MI). All chemicals were used as received without further purification. Electrochemical measurements were made using a potentiostat (CHI 1207A, CH Instruments, Austin, TX) at room temperature (22 ± 1 °C). A digital camera (12.1 megapixels, PowerShot SD960 IS), which was used to obtain pictures, was purchased from Canon.

### Wax screen-printing method

For screen-printing, a mask was created using CorelDraw and printed on a transparency film using a laser printer. Black areas of the mask generate a hydrophobic area on the paper, while colorless areas yield hydrophilic features. The transparency is then used to create the screens at a local screen-printing shop. Solid wax was rubbed through the screen (200 mesh of nylon on an aluminium frame) onto the paper. The printed wax was then melted on a hot plate at 100 °C for 60 s, absorbing into the paper to form hydrophobic barriers (Fig. 1). The patterned paper was ready for use after removing the paper from the hot plate and allowing it to cool to room temperature (<10 s). The screen was placed on tissue paper on a hot plate and heated for 60 s to remove the residual wax.

### Study of molten wax spreading in paper

In the melting step, wax on the paper surface melts and spreads both vertically and horizontally into the paper. To determine the extent of wax spreading, the melting temperature and time were varied from 100–120 °C and 10–60 s, respectively, and resulted in hydrophobic barrier widths of 200–1200 μm. After red food dye was dropped onto the patterned paper, the final width of the hydrophobic barriers was measured by first capturing a digital image and then converting this to size using Adobe Acrobat™. These widths were compared to the widths of the printed masks, and a simple linear equation was generated to select the optimal melting temperature and time.

### Wax screen-printing resolution

To determine the resolution of our method, the final widths of hydrophobic barrier and hydrophilic channel were studied in the range of 1200–1800 μm and 550–1000 μm, respectively at the optimal melting temperature and time. After fabrication, red food dye was added to the paper devices to visualize the hydrophobic and hydrophilic properties.

### Applications

To evaluate the impact of reagent residues on the background signal in paper microfluidics, the BCA assay was used. Results generated on paper devices patterned both by our method and the photolithographic methods were compared. A solution of 0.5 μL each of BCA and $Cu^{2+}$ was dropped at the colorimetric test zone. The paper was then allowed to dry at room temperature for 10 min. For analysis, 12 μL of potassium phosphate buffer or uric acid solution were added and flowed to the measurement zone.

The utility of μPADs fabricated by the wax screen-printing was demonstrated using electrochemical and colorimetric detection for glucose and total iron using the design shown in Fig. S1†. Electrodes were constructed on paper devices using a previously reported screen-printing method.[5,8] Glucose oxidase (1 μL of 645 U $mL^{-1}$ solution) was added to the electrode region. Ascorbic acid (0.5 μL of 1 mM solution) and 1,10-phenanthroline

 

(0.5 μL of 0.25 M solution) were spotted in the colorimetric test zone for total iron detection.[17] The paper was allowed to dry at room temperature for 10 min. For analysis, 12 μL of a standard or sample solution were dropped onto the colorimetric test zone and subsequently flowed to the electrochemical test zone. Direct current chronoamperometry was used for analysis at the screen-printed carbon Prussian Blue-mediated electrode. The sampling rate for all chronoamperometric analyses was 10 Hz. Additionally, the red color intensity relating to the concentration of total iron was measured using Adobe Photoshop™.

### Human serum sample

Human control serum samples (levels 1 and 2) were obtained from Pointe Scientific (Canton, MI). Levels of analytes were provided by the supplier. All samples were analyzed using electrochemical and colorimetric detection for μPADs after protein precipitation with 1.4 M hydrochloric acid (HCl) and 10% (w/v) trichloroacetic acid. For the protein precipitation, 3 mL of sample were added to 1 mL HCl and heated in a water bath at 100 °C for 5 min. After cooling, 2 mL of 10% trichloroacetic acid were added and the resulting suspension was centrifuged at 14 500 rpm (Minispin Plus, Eppendorf) for 5 min.[18–20] Supernatant was diluted in 0.1 M potassium phosphate buffer (pH 6) in a 1 : 1 ratio to adjust the solution pH prior to analysis.

## Results and discussion

### Wax screen-printing

Screen-printing is a technique in which a design is generated on a screen of silk or other fine mesh, with blank areas (areas where no transfer is intended) coated with an impermeable film. Patterns are transferred by forcing ink through the mesh onto the printing surface. Screen-printing is well established for the fabrication of biosensors and chemical sensors because of advantages such as miniaturization, versatility, low cost, and the possibility of mass production.[21–23] Various types of printing surfaces can be used including glass, ceramic, paper, and cotton or similar fabrics. The type of ink also depends on the printing surface and the application. Typically, printing materials include liquid inks and dyes. We reported here the use of solid wax as a printing material for screen-printing hydrophobic barriers on paper (wax screen-printing method) as shown in Fig. 1. Wax is environmentally friendly and much cheaper and easier to obtain than photoresist or PDMS. Moreover, our fabrication method is accomplished without the use of a clean room, UV lamp, organic solvents, or sophisticated instrumentation. From previous reports, wax printing needs a wax printer (~$2500 US) but printing screens required for our method are cheap (<$5 US) and widely available around the world.[13] Although hand drawing with a wax pen in the previous report needs only a common hot plate, it lacks the reproducibility and is difficult to fabricate small channels in high-throughput.[24] The major advantage of our method over previous methods is that it requires only a common hot plate (or similar surface) and a common printing screen that can be produced in any place in the world.

### Wax spreading

The melting temperature and time impact the spreading and penetration of wax into paper, playing an important role in the final pattern dimensions. Wax loading in these experiments was controlled by the thickness of the screen itself. It was found that melting times ranging from 10–40 s at 100 and 150 °C were not adequate for wax penetration into the paper (data not shown). Additionally, melting times in the range of 30–60 s at 200 °C can burn the paper. Hence, 50 and 60 s melting time at 100 and 150 °C, as well as 10 s melting time at 200 °C, were considered. A plot of the resulting hydrophobic barrier widths *versus* the line width from the mask is shown in Fig. 2. The slope and intercept of these plots are shown in Table 1. The intercept represents the width of the smallest hydrophobic barrier (~1100 to 1800 μm). The lowest intercept values were seen for 100 °C for 60 s and 200 °C for 10 s indicating these two conditions resulted in lines most similar to the mask line width. Melting conditions of 100 °C for 60 s were chosen as optimal because they maintained the integrity of the printed features better than 200 °C for 10 s. Using the optimal melting temperature and time, the resulting width of hydrophobic barriers ($W_{RB}$) was calculated using the linear equation $W_{RB} = 1.081\ W_{PB} + 1136.3$, where $W_{PB}$ is the printed line width. The resulting width of hydrophilic channels ($W_{RC}$) was then calculated with eqn (1) and (2), where $L$ is the length of wax spreading from the original wax line, and $W_{PC}$ is the printed width of the channel. Fig. S2† demonstrates these variables in a schematic.

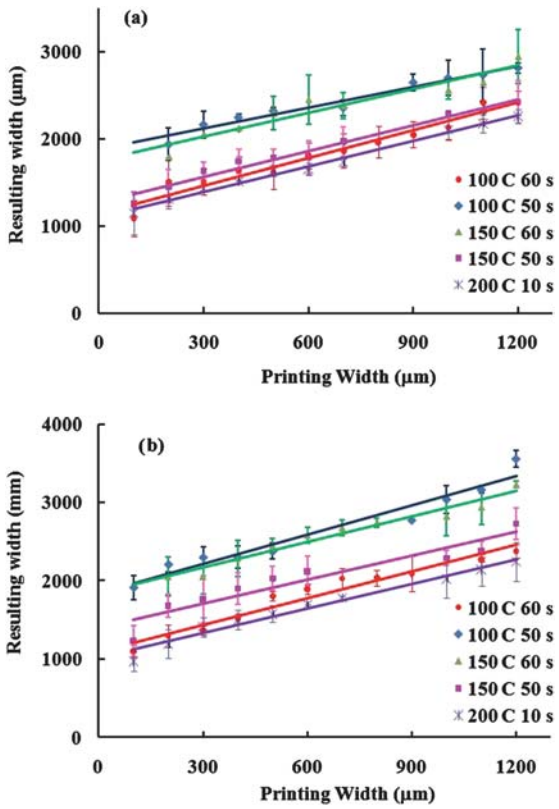


**Fig. 2** Plot of the width of the resulting hydrophobic barriers after melting the wax as a function of the printed width line of wax in (a) front and (b) back of paper devices.

**Table 1** Slope, intercept and $R^2$ of the linearity curve and the matching percentage of slope and intercept between hydrophobic barrier width at front and back of paper devices

| | Slope | | Intercept | | $R^2$ | | % Matching | |
|---|---|---|---|---|---|---|---|---|
| Time : melting temperature | Front | Back | Front | Back | Front | Back | Slope | Intercept |
| 50 s : 100 °C | 0.961 | 1.250 | 1786.1 | 1835.9 | 0.978 | 0.947 | 76.9 | 97.3 |
| 60 s : 100 °C | 1.081 | 1.071 | 1136.3 | 1128.0 | 0.984 | 0.981 | 100.9 | 100.7 |
| 50 s : 150 °C | 1.018 | 1.067 | 1243.8 | 1382.5 | 0.985 | 0.937 | 95.4 | 90.0 |
| 60 s : 150 °C | 1.145 | 1.118 | 1630.1 | 1826.2 | 0.939 | 0.979 | 102.4 | 89.3 |
| 10 s : 200 °C | 0.996 | 1.050 | 1090.6 | 1012.6 | 0.995 | 0.971 | 94.9 | 107.7 |

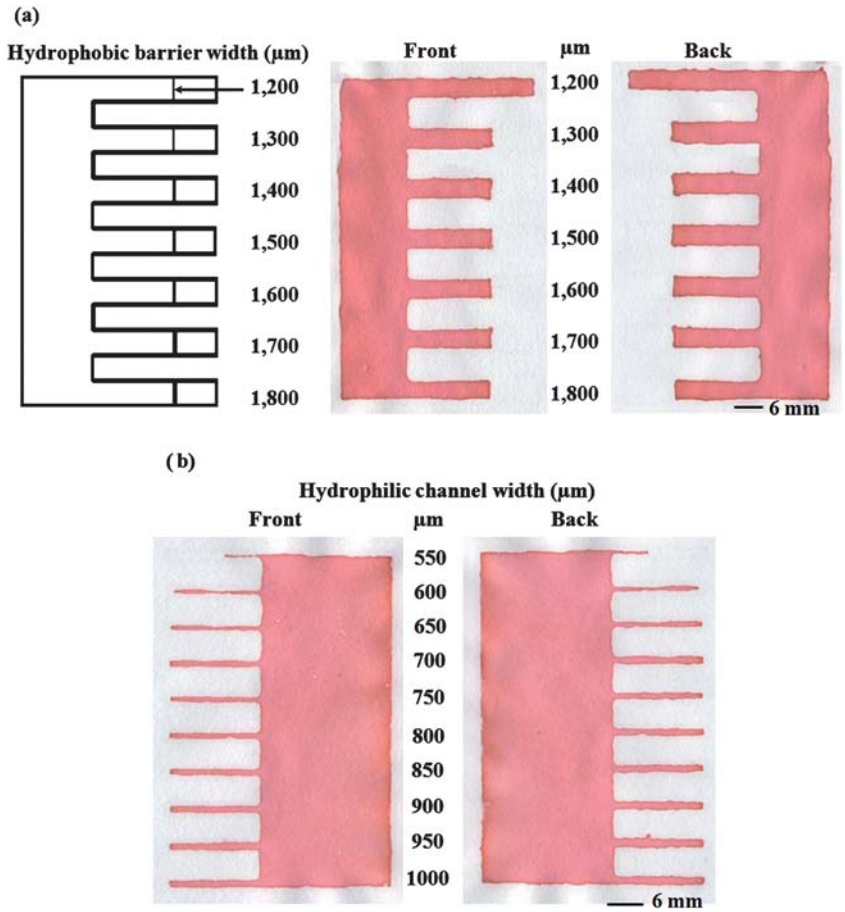


**Fig. 3** Resolution of the wax screen-printing method showing (a) the smallest hydrophobic barrier width and (b) the smallest hydrophilic channel width.

$$2L = W_{RB} - W_{PB} \quad (1)$$

$$W_{RC} = W_{PC} - 2L \quad (2)$$

### Wax screen-printing resolution

2At the optimal melting temperature and time, the width of the hydrophobic barrier from 1200 to 1800 μm was studied in steps of 100 μm (Fig. 3a) to demonstrate the resolution of this method. A minimum hydrophobic barrier of 1300 ± 104 μM was determined. The width of the hydrophilic channel from 550 to 1000 μm in 50 μm steps was also studied (Fig. 3b). The smallest channel width allowing solution to flow the entire length of a 12 mm channel was found to be 650 ± 71 μm ($n = 10$ for inter-batch of fabrication) (Fig. 3b). The resolution of our method is currently limited by the thickness, porosity, and orientation of paper fibers as well as the smallest features printable on the screen. Here, only Whatman #1 filter paper (180 μm thickness and 11 μm particle retention rating at 98% efficiency) was used; and it is anticipated that some differences will exist for different printing surfaces. Moreover, we studied the reproducibility of channel and barrier widths at the minimum of hydrophobic barrier and hydrophilic channel (>650 and 1300 μm, respectively). The result shows that the relative standard deviation was less than 11% for all channel and barrier widths.

 

## Applications

To demonstrate the effect of the patterning method on the background signal, a total reducing agent analysis using the reaction between bicinchoninic acid (BCA) and $Cu^{1+}$ as a model was used. $Cu^{2+}$ ion is converted to $Cu^{1+}$ by the reducing agents such as uric acid, vitamin E and ascorbate. $Cu^{1+}$ is chelated with BCA giving an intense violet color, proportional to the total reducing agents. No reaction was seen when the BCA and $Cu^{2+}$ solution was carried out on devices patterned with the wax screen printing method; however, a positive result was obtained when using paper devices patterned by photolithography (Fig. 4). This result indicates that the patterning method can give rise to false signals. It has been shown in a previous report that photoresist residues can also interfere with amperometric detection in paper-based microfluidic devices.[7]

In order to evaluate the utility of wax screen-printed μPADs, the simultaneous determination of glucose and total iron in control human serum samples was performed. The design of the paper device is shown in Fig. S1†. Total iron was analyzed by a colorimetric method involving the formation of a red-colored complex between 1,10-phenanthroline and iron(II). The color intensity increased with iron concentration (Fig. 5a). Color intensity calibrations were done using Adobe Photoshop™ in gray scale mode using 1200 pixel area in a circle shape within a range of 0–200 μM, generating coefficients of determination ($R^2$) greater than 0.999 (Fig. S3†) whereas 1000 μM of total iron gave a constant color intensity. The relative standard deviations of all iron concentrations were less than 17% ($n = 3$), demonstrating acceptable reproducibility for this type of device. Improvements in the reproducibility could potentially be achieved using a reaction that generated a more intense color. For glucose determination, Prussian Blue modified carbon working electrodes were used to detect hydrogen peroxide generated from the reaction between glucose and glucose oxidase. The devices were initially characterized using cyclic voltammetry. Fig. S4† clearly shows a larger cathodic peak in the presence of hydrogen peroxide and glucose relative to the background electrolyte. The catalytic reaction occurs in a low potential region (−0.2 to 0 V *versus* on-paper Ag/AgCl). Next, a linear calibration curve was obtained using chronoamperometry at −0.2 V and 0–5 mM glucose ($Y = -1.009X + 0.151$, $R^2 = 0.9925$, %RSD of all glucose conc. ≤12% ($n = 3$)) as shown in Fig. 5b.

Finally, the glucose and total iron concentration in control human serum samples were determined simultaneously. Control serum samples are used to validate clinical assays. After sample preparation, the final sample solution was diluted by a factor of four giving final concentrations of total iron in human serum levels 1 and 2, and level 2 spiked with 200 μM of iron was 3.5, 12, and 62 μM, respectively. A correlation of the color intensity between the standard iron solution and iron in serum sample was observed visually and

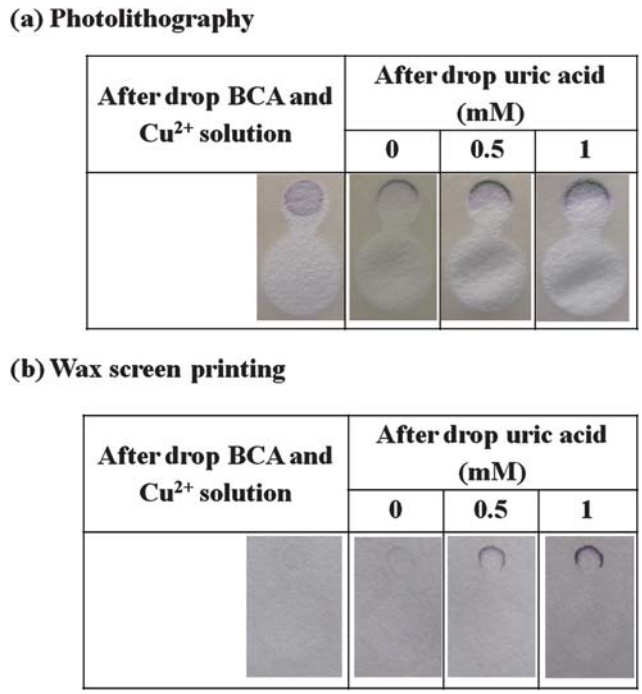


**Fig. 4** Cross-reaction test with BCA assay: (a) photolithography and (b) paper devices fabricated by our method.

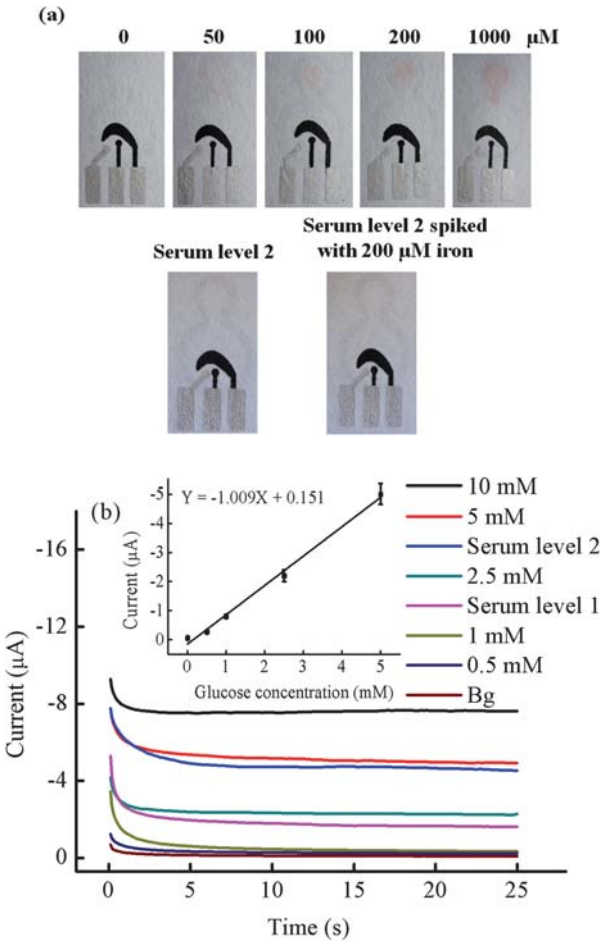


**Fig. 5** (a) Photographs of the result for the total iron analysis using colorimetric method. (b) Chronoamperograms of glucose (0–10 mM) determination at −0.2 V *versus* an on-chip Ag/AgCl. The calibration plot of anodic currents at 20 s of sampling time for determination of three analytes are shown in the inset, $n = 3$.

**Table 2** Determination of glucose and total iron in control samples

| | Human serum level 1 | | Human serum level 2 | |
|---|---|---|---|---|
| Analyte | Certified value | Proposed method | Certified value | Proposed method |
| Glucose concentration/ mM ± SD[a] | 5.6 ± 0.4 | 5.2 ± 0.5 | 16.8 ± 1.7 | 18.4 ± 2.2 |
| Iron concentration/ μM ± SD[a] | 14 ± 3 | ND[b] | 49 ± 9 | 44 ± 6 |

[a] SD: standard deviation ($n = 3$). [b] ND: not detectable.

measured by Adobe Photoshop™. The color intensity of the iron reaction at serum sample level 1 did not show a significant difference visually (data not shown). A linear calibration curve generated from gray scale measurements was used to interpret the iron in serum level 2 and spiked level 2 (Fig. S3†) samples. The serum level 2 and spiked level 2 samples were determined to contain 11 ± 2 and 58 ± 6 μM iron (Fig. 5a). The recovery of iron was determined to be 88–92% ($n = 3$). For the glucose test, the final concentration of level 1 and 2 samples after sample preparation was 1.4 ± 0.1 and 4.2 ± 0.4 mM, respectively. The results of both glucose and iron converted to their original concentrations are shown in Table 2. Using the paired *t*-test, no significant differences were found at the 95% confidence level between our measurements and the known values.

## Conclusions

Here, we demonstrate a wax screen-printing method for fabricating μPADs. The wax screen-printing method is rapid, inexpensive, simple, and suitable for developing countries. A linear equation between the width of a hydrophobic barrier and the width of the printed line was used to predict the width of a hydrophobic barrier and a hydrophilic channel from the initial printed mask. Moreover, the screen-printing method does not suffer from problems of interference from residues remaining in the hydrophilic channel after fabrication. Finally, the fabrication method was shown to be useful for both colorimetric and electrochemical detection methods, and was applied to the simultaneous determination of glucose and total iron in biologically relevant samples.

## Acknowledgements

WD gratefully acknowledges the financial support from the Thailand Research Fund through the Royal Golden Jubilee PhD Program (grant no. PHD/0039/2548). OC also like to thank the Thai Government Stimulus Package 2 (TK2555), under the Project for Establishment of Comprehensive Center for Innovative Food, Health Products and Agriculture (PERFECTA). CSH acknowledges support for a Fulbright Scholar Award from the Thailand–US Educational Foundation.

## References

1 A. W. Martinez, S. T. Phillips, G. M. Whitesides and E. Carrilho, *Anal. Chem.*, 2009, **82**, 3–10.
2 A. W. Martinez, S. T. Phillips, M. J. Butte and G. M. Whitesides, *Angew. Chem., Int. Ed.*, 2007, **46**, 1318–1320.
3 A. W. Martinez, S. T. Phillips, E. Carrilho, S. W. Thomas, H. Sindi and G. M. Whitesides, *Anal. Chem.*, 2008, **80**, 3699–3707.
4 A. W. Martinez, S. T. Phillips, B. J. Wiley, M. Gupta and G. M. Whitesides, *Lab Chip*, 2008, **8**, 2146–2150.
5 W. Dungchai, O. Chailapakul and C. S. Henry, *Anal. Chem.*, 2009, **81**, 5821–5826.
6 Z. Nie, C. A. Nijhuis, J. Gong, X. Chen, A. Kumachev, A. W. Martinez, M. Narovlyansky and G. M. Whitesides, *Lab Chip*, 2010, **10**, 477–483.
7 R. F. Carvalhal, M. Simão Kfouri, M. H. de Oliveira Piazetta, A. L. Gobbi and L. T. Kubota, *Anal. Chem.*, 2010, **82**, 1162–1165.
8 A. Apilux, W. Dungchai, W. Siangproh, N. Praphairaksit, C. S. Henry and O. Chailapakul, *Anal. Chem.*, 2010, **82**, 1727–1732.
9 D. A. Bruzewicz, M. Reches and G. M. Whitesides, *Anal. Chem.*, 2008, **80**, 3387–3392.
10 K. Abe, K. Suzuki and D. Citterio, *Anal. Chem.*, 2008, **80**, 6928–6934.
11 X. Li, J. Tian, T. Nguyen and W. Shen, *Anal. Chem.*, 2008, **80**, 9131–9134.
12 E. M. Fenton, M. R. Mascarenas, G. P. López and S. S. Sibbett, *ACS Appl. Mater. Interfaces*, 2008, **1**, 124–129.
13 E. Carrilho, A. W. Martinez and G. M. Whitesides, *Anal. Chem.*, 2009, **81**, 7091–7095.
14 M.-H. Chiu, H. Wu, J.-C. Chen, G. Muthuraman and J.-M. Zen, *Electroanalysis*, 2007, **19**, 2301–2306.
15 H. Tao, Z. Xian-En, Z. Zhi-Ping and C. Li-Qun, *Electroanalysis*, 2000, **12**, 868–870.
16 F. Ricci, A. Amine, C. S. Tuta, A. A. Ciucu, F. Lucarelli, G. Palleschi and D. Moscone, *Anal. Chim. Acta*, 2003, **485**, 111–120.
17 A. Apilux, W. Dungchai, W. Siangproh, N. Praphairaksit, C. S. Henry and O. Chailapakul, *Anal. Chem.*, 2010, **82**, 1727–1732.
18 R. E. Peterson, *Anal. Chem.*, 1953, **25**, 1337–1339.
19 B. Zak, *Clin. Chim. Acta*, 1958, **3**, 328–334.
20 R. Ryall and J. Fielding, *Clin. Chim. Acta*, 1970, **28**, 193–202.
21 O. D. Renedo, M. A. Alonso-Lomillo and M. J. A. Martínez, *Talanta*, 2007, **73**, 202–219.
22 M. Tudorache and C. Bala, *Anal. Bioanal. Chem.*, 2007, **388**, 565–578.
23 K. C. Honeychurch and J. P. Hart, *TrAC, Trends Anal. Chem.*, 2003, **22**, 456–469.
24 Y. Lu, W. Shi, L. Jiang, J. Qin and B. Lin, *Electrophoresis*, 2009, **30**, 1497–1500.

 